

Granular elasticity: General considerations and the stress dip in sand pilesDmitry O. Krimer,¹ Michael Pfitzner,² Kurt Bräuer,¹ Yimin Jiang,^{3,1} and Mario Liu^{1,*}¹*Theoretische Physik, Universität Tübingen, 72076 Tübingen, Germany*²*Universität der Bundeswehr München, 85579 Munich, Germany*³*School of Physics Science and Technology and State Key Laboratory for Powder Metallurgy, Central South University, Changsha 410083, China*

(Received 27 March 2006; revised manuscript received 28 June 2006; published 27 December 2006)

Granular materials are predominantly plastic, incrementally nonlinear, preparation-dependent, and anisotropic under shear. Nevertheless, their static stress distribution is well accounted for, in the whole range up to the point of failure, by a judiciously tailored isotropic nonanalytic elasticity theory termed *granular elasticity*. The first purpose of this paper is to carefully expound this view. Then granular elasticity is employed to consider the stress distribution in two-dimensional sand piles (or sand wedges). Starting from a uniform density, the pressure at the bottom of the pile is found to show a single central peak. It turns into a pressure dip, if some density inhomogeneity, with the center being less compact, is assumed. These two pressure distributions are remarkably similar to recent measurements, made in piles obtained, respectively, by rainlike pouring and funneling. In an accompanying paper, the stress distributions in silos and under point loads, calculated using the same method, are also found to agree with experiments.

DOI: [10.1103/PhysRevE.74.061310](https://doi.org/10.1103/PhysRevE.74.061310)

PACS number(s): 45.70.-n

I. INTRODUCTION

Static stress distribution is useful information for any system and an important result of continuum mechanics. Therefore, the fact that for a system as familiar as granular materials no universally accepted and geometry-independent theory for stress calculation exists [1] calls for efforts to amend the situation.

One part of stress calculation is generally accepted and comprises of the force balance, or the static part of momentum conservation. Neglecting gravitation, it reads [2]

$$\nabla_j \sigma_{ij} = 0, \quad (1)$$

where σ_{ij} is the symmetric stress tensor, with six independent components. As this is a vector equation with only three components, three additional equations are needed to uniquely determine σ_{ij} . For elastic media, such closure conditions are obtained by considering the medium's response to deformation. In granular systems, no commonly accepted closure condition exists.

Using general physical principles and well-known experimental results, we argue in this paper why a carefully tailored elasticity remains appropriate, and where its limitations are. In addition, we suggest an explicit elastic energy, and derive a curtailed stress-strain relation to serve as the closure condition for granular systems. This expression contains only two material parameters, one accounting for total stiffness, the other for the Coulomb angle. Although minimalistic, it proves well capable of accounting for many features of granular statics, see Sec. VI. This closure condition is employed both in Sec. VII of this and in an accompanying paper [3], to compute the stress distribution, in the classic geometries of silos, point loads, and sand piles. Our goal hereby is not so much to give a quantitative account, more to

validate the general idea of this specific elastic approach, showing that the presented stress-strain relation is capable of accounting for the important, qualitative features in these geometries. Happily, as we shall see, the agreement found frequently exceeds this goal.

After a brief discussion of classical elasticity and a proof that force balance holds only in equilibrium (in Secs. II and III), the peculiarities of granular stress are presented in Sec. IV, and existent ways to account for them commented upon in Sec. V. Section VI presents GE (granular elasticity), the elastic theory tailored for granular materials.

II. CLASSICAL ELASTICITY

The energy w of a solid increases with deformation, or a nonuniform displacement U_i . Quantifying the deformation with the strain u_{ij} , where $u_{ij} = \frac{1}{2}(\nabla_i U_j + \nabla_j U_i)$ for small displacements, and taking the deformation energy density as $w = w(u_{ij})$, the stress is given by [2],

$$\sigma_{ij}(u_{k\ell}) = -\partial w / \partial u_{ij}. \quad (2)$$

Since this stress-strain relation gives the stress σ_{ij} as a function of the displacement U_i (six versus three components), it represents three closure conditions that suffice to close Eq. (1). Inserting Eq. (2) into (1) yields three second-order differential equations for the variables U_i ,

$$(\partial \sigma_{ij} / \partial u_{k\ell}) \nabla_j u_{k\ell} = 0, \quad (3)$$

which may be solved for any geometry with appropriate boundary conditions. Inserting the resultant displacement field into Eq. (2) yields the stress distribution.

There are a number of specific expressions for the energy w . Simplest is the case of isotropic linear elasticity (ILE). Denoting $\Delta \equiv -u_{\ell\ell}$, $u_s^2 \equiv u_{ij}^0 u_{ij}^0$, $u_{ij}^0 \equiv u_{ij} - \frac{1}{3} u_{\ell\ell} \delta_{ij}$, it is given as

$$w = \frac{1}{2} K \Delta^2 + \mu u_s^2, \quad \sigma_{ij} = K \Delta \delta_{ij} - 2\mu u_{ij}^0, \quad (4)$$

*Electronic mail: mliu@uni-tuebingen.de

$$\partial\sigma_{ij}/\partial u_{k\ell} = \left(\frac{2}{3}\mu - K\right)\delta_{ij}\delta_{k\ell} - \mu(\delta_{ik}\delta_{j\ell} + \delta_{jk}\delta_{i\ell}), \quad (5)$$

where $K, \mu > 0$ are two material constants, which vary from material to material, but do not depend on geometry or external forces.

Next are the many familiar examples for anisotropic linear elasticity (ALE), classified according to symmetry. Rhombic symmetry for instance allows nine different material constants, instead of the two above. The stress-strain relations is always a straight line, same as in ILE, but the slope varies with direction. In other words, the stiffness tensor, $M_{ijk\ell} \equiv \partial\sigma_{ij}/\partial u_{k\ell}$, although independent of stress or strain, no longer sports the isotropic appearance of Eq. (5).

A less common example is isotropic nonlinear elasticity (INE), with an energy that is a more general function of Δ, u_s than Eq. (4). (It may in addition depend on $u_3 \equiv \sqrt[3]{u_{ij}^0 u_{jk}^0 u_{ki}^0}$.) The resultant stress-strain relation is no longer a straight line, though the incremental relation of course remains linear,

$$\delta\sigma_{ij} = (\partial\sigma_{ij}/\partial u_{k\ell})\delta u_{k\ell} \equiv M_{ijk\ell}\delta u_{k\ell}. \quad (6)$$

Because the stiffness tensor $M_{ijk\ell}$ is strain- (or stress-) dependent, and the given stress may be anisotropic, the slope will vary with direction, displaying an *incremental anisotropy* that may appear quite similar to ALE. Still, both types of anisotropy are qualitatively different, as ALE is *inherently anisotropic*, while INE displays *stress-induced anisotropy*.

Assuming elasticity may indeed be successfully applied to granular systems, the following points are useful to keep in mind: (i) Given the randomness, uniform sand should be quite isotropic in the limit of vanishing stresses—turning slowly anisotropic only as the stress increases. Therefore, granular anisotropy should be primarily stress induced, making INE a suitable candidate for granular elasticity. (ii) Some inherent “fabric anisotropy” is not inconceivable, although the one ready possibility, partial ordering or some degrees of “crystallization” at higher hydrostatic pressure, is likely only for monodisperse grains. (iii) The following scenario may lead to false evidences for fabric anisotropy: Assuming the elastic coefficients are density dependent, and that the density is nonuniform, say with a gradient along x . Then, clearly, this system will appear anisotropic even for vanishing stresses. GE, or granular elasticity, as presented in Sec. VI is a specific form of INE. It accounts for shear-induced anisotropy and density inhomogeneity, but does not address fabric anisotropy.

III. FORCE BALANCE AND EQUILIBRIUM

Although the validity of force balance Eq. (1) in static circumstances is quite obvious, it is useful (especially for the description of dynamic processes) to realize that the force balance represents an equilibrium condition that, similar to the constancy of temperature, states the entropy is maximal with respect to variations of the displacement: Taking the energy density w as a function of the entropy density s and the strain u_{ij} ,

$$dw = Tds - \sigma_{ij}du_{ij}, \quad (7)$$

we vary the entropy $\int d^3rs$ at given energy $\int d^3rw$ and fixed displacement at the medium’s surface. Taking $1/T_0$ as a

Lagrange parameter, denoting the surface element as da_i , and noticing $\sigma_{ij}du_{ij} = \sigma_{ij}d\nabla_i U_j$, we have

$$\begin{aligned} \delta \int \left(s - \frac{w}{T_0} \right) d^3r &= \int \left(\frac{1}{T} \delta w + \frac{\sigma_{ij}}{T} \delta u_{ij} - \frac{1}{T_0} \delta w \right) d^3r \\ &= \int \left[\left(\frac{1}{T} - \frac{1}{T_0} \right) \delta w - \nabla_i \left(\frac{\sigma_{ij}}{T} \right) \delta U_j \right] d^3r \\ &\quad + \oint \frac{\sigma_{ij}}{T} \delta U_i da_i, \end{aligned}$$

where the last term vanishes because $\delta U_i \equiv 0$ at the surface. If the entropy is maximal, the whole expression vanishes. And since δw and δU_j vary independently, this implies $T = T_0$, and more importantly, $\nabla_i \sigma_{ij} = 0$. These conclusions are quite general, and not confined to elastic media. In granular materials, it remains true that the equilibrium macrostate (for which the force balance is satisfied everywhere) has the largest number of microscopic configurations, many more than those nonequilibrium macrostates, in which force balance is occasionally violated.

Since force balance is universally accepted to hold in jammed systems, and it implies entropy is maximal with respect to variations of the displacement, the strain field u_{ij} cannot possibly be the one that gets stuck when the stress field σ_{ij} is frozen in by jamming grains. Some other macroscopic variables on which the stress depends must get stuck (e.g., the density, see the discussion below, in Sec. IV), rendering stresses preparation dependent.

Among physicists, a different interpretation has gained some credence: Dependence on preparation is a consequence of granular systems prevented by jamming from exploring the phase space. For instance, although the potential energy of a grain somewhere in a sand pile is orders of magnitude larger than the ambient temperature, it will remain in that position forever if unperturbed. The phase space consists of many different microscopic granular configurations, each with a unique position, orientation and deformation of every single grain. These are not explored by the grains, and no averaging takes place. Stress measurements on systems differently prepared is probing the grains stuck in different configurations.

We believe that this point of view mixes microscopic and macroscopic arguments impermissibly. In fact, if it really holds water, stress—along with all other granular properties—can only be calculated using a microscopic theory, in which the configuration is specified. No macroscopic description, given by a handful of partial differential equations, is possible, because it is always a result of averaging, which alone reduces the complexity of the system to a few macroscopic variables. This would leave molecular dynamic simulation the only possibility to account for granular behavior. Some engaging in granular simulation do appear tempted by this view, believing that any macroscopic granular theory is necessarily haphazard, incapable of covering the whole range of granular phenomena. But along with many in physics and most in soil mechanics, we shall take the possibility of a macroscopic theory for granted. (Of course, no macroscopic granular theory can be as accurate as, say, the

Navier-Stokes equations for water, because the grains are much larger than atoms and molecules. Fluctuations around averages may always be detectable—more easily so in small samples with large grains.)

IV. GRANULAR STRESS

All three types of elasticity theory ILE, ALE, and INE, allow one to calculate the stress distribution generally, by solving Eq. (1) for specific geometry and boundary conditions. Our goal is to find a similarly complete procedure for calculating granular stress distributions. An obvious first question is whether employing elasticity would exclude two important granular characteristics: *incremental nonlinearity* and *preparation dependence of the stress*.

Incremental nonlinearity, a striking feature of granular systems, is often cited in support of the view that sand is not elastic [4]. Given any unique stress-strain relation, $\sigma_{ij}(u_{kl})$, Eq. (6) or “incremental linearity” holds. In sand, the relation between $\delta\sigma_{ij}$ and δu_{kl} is incremental nonlinear, as it depends strongly on the sense of change, whether the stress is being increased or decreased, whether the system is being *loaded* or *unloaded*.

We do not believe that this rules out elasticity: In granular media, grains may slide and roll, in addition to being compressed and sheared. The displacement associated with the former is frequently orders of magnitude larger, but only the latter, the displacement associated with deforming the grains, stores up energy and maintains a stress. Sliding and rolling are irreversible, dissipative processes, they heat up the system, but do not lead to reversible energy storage. So, denoting the total strain field as ε_{ij} , it has two contributions, $\varepsilon_{ij} = u_{ij} + u_{ij}^p$, the reversible elastic one, u_{ij} , and the irreversible plastic one, u_{ij}^p . Granular energy is a function of the elastic strain, $w = w(u_{ij})$, with the stress given by $\sigma_{ij} = -\partial w / \partial u_{ij}$, an expression we may refer to as an *elastic-strain-stress relation*. The associated incremental relation is linear, as Eq. (6), and *incremental nonlinearity* arises because it is the total strain $\delta\varepsilon_{kl}$ that is observed.

A small quantity often overwhelmed by its plastic counterpart, the elastic strain is hard to measure directly. Nevertheless, the elastic-strain-stress relation is quite sufficient to close the force balance, Eq. (1). This is very fortunate, as it reduces the notoriously open problem of granular stress calculation to finding an appropriate expression for the energy $w = w(u_{ij})$. Once given, we may solve Eq. (3) for any geometry and boundary conditions, obtaining the stress and the elastic displacement at the same time. Note that the boundary conditions must be given in terms of the proper variables or their spatial derivatives, i.e., either the stress or the elastic displacement, not the perceived total displacement.

Plastic contributions do not always dominate. When probing the strain response δu_{ij} to a stress increment $\delta\sigma_{kl}$, the plastic contributions decrease with the amplitude of the increments. This is plausible, because slips become rarer in the limit of vanishing increments; and this is born out by experiments and simulations alike: Kuwano and Jardine observed [5] that keeping the strain increments below 10^{-4} , the stress increments become symmetric and reversible, incrementally

linear. In molecular-dynamic simulations, Alonso-Marroquin and Herrmann found the same behavior [6]: For elastic strains of the order of 10^{-6} , the irreversible plastic contributions are around 10^{-14} , smaller by 8 orders of magnitude. This circumstance is very useful, as it implies that the stiffness tensor M_{ijkl} of Eq. (6),

$$\delta\sigma_{ij} = M_{ijkl} \delta u_{kl} \approx M_{ijkl} \delta\varepsilon_{kl}, \quad (8)$$

is directly accessible by measuring $\delta\varepsilon_{kl}$ for given $\delta\sigma_{ij}$, as a function of the stress. In principle, this allows one to obtain an explicit elastic-strain-stress relation, $\sigma_{ij} = \sigma_{ij}(u_{ij})$, by integrating δu_{kl} over $\delta\sigma_{ij}$. Although the elastic displacement thus obtained will typically be quite different from the actual displacement the granular system underwent to achieve the given stress, this relation is, as already emphasized, well suited to serve as a closure condition for the force balance.

Next, we discuss the *dependence of granular stresses on preparation*. An example is provided in Ref. [7], showing that the stress dip below a sand pile is present if the sand is funneled onto the pile, not if it is poured rainlike from a sieve. The point is, preparation dependence is not ruled out by the elasticity as given above. We shall consider this experiment in Sec. VII, laying out only the general considerations here. First, since force balance Eq. (1) is an equilibrium condition, implying that entropy is maximal with respect to variations of the elastic displacement, see Sec. III, its validity implies that elastic strain fields (associated with the deformation of the grains) do not get stuck when the grains are jammed. So dependence on preparation are due to other macroscopic variables, which do keep their values at preparation and modify the stress accordingly—typically by up to 10%, as different preparations by Refs. [7–10] show.

The density ρ is such a macroscopic variable, as it remembers the preparation and modifies the stress. In granular media, repackaging changes ρ by up to 20%. Once the grains are jammed and the system settled, the packaging, even if nonuniform, will stay. And it is well known that granular systems become stiffer when the grains are more closely packed, implying that the elastic coefficients grow with ρ . [There is also a tiny compressional variation of the density, $\rho = \rho_0(1 + \Delta)$ for given packaging, where ρ_0 is the density without compression. So strictly speaking, it is ρ_0 that maintains its value at preparation. However, with Δ typically of order 10^{-4} , we have $\rho_0 \approx \rho$.] A nonuniform density modifies the force balance

$$\nabla_j \sigma_{ij} = \frac{\partial \sigma_{ij}}{\partial u_{kl}} \nabla_j u_{kl} + \frac{\partial \sigma_{ij}}{\partial \rho} \nabla_j \rho = 0, \quad (9)$$

and quite obviously influences the stress distribution directly.

It is not clear whether density is the only such macroscopic variable. There are some discussions on *fabric anisotropy* or *texture* in the literature, but less on their macroscopic definition, tensorial character, equation of motion, and above all, evidence of their independence. Experimentally, it is possible to detect anisotropy, but difficult to trace its origin, discerning whether it is shear induced, driven by density inhomogeneity, or caused by a third reason. Only in this last case is it necessary to include additional variables. Facing

this situation, the constructive way to proceed is to first assume none is needed. Then compare, as much as possible, theoretical predictions with experimental data. If agreement is found in all cases, one may forget fabric anisotropy. If agreement proves elusive, and some form of fabric anisotropy must be included, this strategy should nevertheless end up giving us better ideas of how large its influence is, perhaps even how to treat it macroscopically.

V. STATE OF STRESS CALCULATION

The existent models for computing granular stresses may be divided into two types, the first consists of explicit relations among stress components and are typically tailored for specific geometries; the second type is given by various elasticity theories. (The difference between both is not in fact qualitative. In essence, the second type also provides relations among stress components, albeit implicit ones.) Both the model of incipient failure (IF) and the Janssen model belong to the first type. IF starts from the assumption that the system is nowhere far from yield, and takes the stress components as related by the Coulomb yield condition [12]. In two dimensions, this one condition suffices to close the force balance Eq. (1), leaving the Coulomb yield angle φ as the only material parameter. The Janssen model, relevant for silos, takes the ratio between the horizontal and vertical stress, $k_J = \sigma_{rr}/\sigma_{zz}$, as a spatial constant [13]. Regarding k_J as a material parameter, this condition closes the force balance and determines the stress of a two-dimensional silo. (For cylindrical silos, more conditions are needed, typically given as $\sigma_{rr} = \sigma_{\theta\theta}$, or that σ_{zz} does not depend on r .) Remarkably, an empirical formula (frequently attributed to Jaky) relates k_J and φ as $k_J = 1 - \sin \varphi$, making φ again the only material parameter. Generalizing the basic idea of these engineering models, Wittmer, Claudin, Cates, and Bouchaud postulate three algebraic relations among stress components, called FPA, sufficient for closing the force balance in three dimensions [14]. FPA reproduces the stress dip in sand piles, but it also predicts that a point force on top of a layer of sand produces two pressure peaks at its bottom—although only one is observed [8–10]. See Ref. [10] for a well rounded review of the question whether the stress propagation is elliptic or hyperbolic, including many worthy references; see also the simulation by Goldenberg and Goldhirsch [15], and the data on photoelastic stress measurement [16].

ILE (isotropic linear elasticity) is employed in soil mechanics to obtain approximate stress distributions, primarily because of its simplicity. To force agreement with measured stresses, the elastic constants, K and μ , are taken as fit parameters. This is inadequate and produces unphysical consequences. Sand is incrementally anisotropic and frequently closed to yield, neither is accounted for. Taking K , μ as fit parameters will work when one has sufficiently narrow focuses, such as on the normal stress at the bottom. But the same Poisson ratio may not account for other stress components, away from the bottom, or in some different geometries. Finally, without prior knowledge of K and μ , or any procedure for calculating them, ILE lacks any predictive power, and is no longer a complete and closed theory. Stress

must first be measured, and then obtained in an inverse process by trial and error.

More recently, Atman *et al.* [10] employ ALE (anisotropic linear elasticity) to account for their results. Measuring the stress response to a point load in a slab of sand, which is either sheared or prepared as avalanche-compacted layers, they follow Otto *et al.* [11] in taking the isotropy of granular textures broken by its preparation—an anisotropic state that is probed by the point load. Accordingly, a number of elastic coefficients were postulated, appropriate for yielding agreement when employed to calculate the stress response to the point load.

Clearly, it would be desirable to find a procedure for calculating these coefficients, quantifying how anisotropy grows with stress, as this would render the model complete and closed. Note INE (isotropic nonlinear elasticity)—including a proper interpretation of the strain as being the elastic part—could do just this: A sheared slab of sand satisfies the force balance $\nabla_j \sigma_{ij} = 0$ (if gravitation is neglected). Adding the point load, the force balance becomes $\nabla_j (\sigma_{ij} + \delta\sigma_{ij}) = 0$, where $\delta\sigma_{ij}$ is the associated stress increment, or $\nabla_j \delta\sigma_{ij} = 0$. If the point load is small enough, we may expand $\delta\sigma_{ij} \approx M_{ijk\ell} \delta u_{k\ell}$, where $M_{ijk\ell} \equiv \partial\sigma_{ij}/\partial u_{k\ell} = -\partial^2 w/\partial u_{ij}\partial u_{k\ell}$ is a function of σ_{ij} , an anisotropic quantity if σ_{ij} is. But $\delta\sigma_{ij} = M_{ijk\ell}(\sigma_{ij}) \delta u_{k\ell}$ is essentially the equation (1) that Atman *et al.* employed to evaluate their stress. In Sec. VI, a suitable energy w for calculating $M_{ijk\ell}$ is suggested, with a detailed comparison carried out in the accompanying paper [3].

Although the anisotropy is similar, the slab of sand consisting of avalanche-compacted layers is not exposed to external stresses and must be understood and calculated differently. We suspect the anisotropy may be a result of density inhomogeneity created by the avalanches, but a verification is only possible if the density field is known.

VI. GRANULAR ELASTICITY

In choosing an energy from INE, we aim for simplicity and generality, looking for broad agreement rather than perfect account of some specific experiments. The following energy density [17] suits our purpose well:

$$w = \sqrt{\Delta} (\mathcal{B} \frac{2}{5} \Delta^2 + \mathcal{A} u_s^2) = \mathcal{B} \sqrt{\Delta} (\frac{2}{5} \Delta^2 + u_s^2/\xi), \quad (10)$$

where \mathcal{A} , $\mathcal{B} > 0$ (with $\xi \equiv \mathcal{B}/\mathcal{A}$) are two strain-independent coefficients. The nonanalyticity $\sim \sqrt{\Delta}$ accounts for the nontensile character of granular systems and forces the compression Δ to stay positive everywhere in an actual calculation. (In linear elasticity, in contrast, negative values for Δ is quite common.) Writing the stress in the familiar form of ILE,

$$\sigma_{ij} = -\partial \varepsilon / \partial u_{ij} = K \Delta \delta_{ij} - 2\mu u_{ij}^0, \quad (11)$$

the bulk and shear moduli are given as strain-dependent functions,

$$K = \mathcal{B} \sqrt{\Delta} (1 + \frac{1}{2} u_s^2/\Delta^2 \xi), \quad \mu = \sqrt{\Delta} \mathcal{B}/\xi. \quad (12)$$

The coefficient \mathcal{B} accounts for overall rigidity, it increases with the density ρ , or equivalently, decreases with the void ratio $e \equiv \rho_g/\rho - 1$, where ρ_g is the bulk density of the

granular material. Sound velocity was measured by Hardin and Richart [19], who found it linear in the void ratio, $c \sim 2.17 - e$. Given Eqs. (11) and (12), the velocity of sound is $c \sim \sqrt{B/\rho}$. Setting $\sqrt{B/\rho} \sim 3.17 - \rho_g/\rho$, or $B \sim (3.17 - \rho_g/\rho)^2(\rho/\rho_g)$, we have

$$B = B_0 \times (2.17 - e)^2 / [1.3736(1 + e)], \quad (13)$$

where B_0 (the value of B at $e=0.66$) is a material constant that is small for rubber grains, large for granite ones, and around 8500 MPa for Ham river sand, see Ref. [18].

The term $B\sqrt{\Delta}$ in K is of course reminiscent of the Hertz contact, though it is not clear to us under what microscopic conditions Eq. (12) holds, whether Hertz contacts are necessary. Perhaps this connection is less important, because whether a stress-strain relation is true, or false, is determined simply by the sum of its macroscopic ramifications. In accounting for granular peculiarities, including volume dilatancy, shear-induced anisotropy and yield, it is in fact the second term $\sim u_s^2/\Delta^{1.5}$ that is especially useful: The energy w is convex only for

$$u_s/\Delta \leq \sqrt{2\xi}, \quad (14)$$

and no elastic solution is possible beyond it. Writing this inequality in terms of stresses, and denoting $P \equiv \frac{1}{3}\sigma_{\ell\ell}$, $\sigma_s \equiv \sqrt{\sigma_{ij}^0\sigma_{ij}^0}$, $\sigma_{ij}^0 \equiv \sigma_{ij} - P\delta_{ij}$, we obtain the (Drucker-Prager variant of the) Coulomb condition

$$\sigma_s/P \leq \sqrt{2\xi}. \quad (15)$$

A thermodynamic energy must be a convex function of the state variables to ensure stability. This is why compressibility and specific heat are always positive. [Being a quadratic function of Δ and u_s , the energy of ILE, Eq (4), is always convex.] There is an instructive analogy between the granular stress-strain relation, Eqs. (11) and (12), and the van der Waals equation of state for real gases. The Boyle's law is stable everywhere while the van der Waals equation has a nonphysical zone, the liquid-gas instability, in which the compressibility is negative. Similarly, the Hooke's law of Eq. (4) is stable everywhere, but the granular stress-strain relation has a forbidden region, that beyond yield. Since $\partial P/\partial \Delta|_{\sigma_s} \geq 0$ is implied by the convexity condition, this forbidden region is also characterized by a negative compressibility. The actual innovation of the van der Waals theory is the fact that the condition for the onset of the liquid-gas transition, instead of being an additional input, is implied by the free energy. Similarly, yield is now a result of elasticity.

Approximating the Coulomb condition Eq. (15) as density independent, we take ξ as the second material constant of our energy w . As a layer of sand on a inclined plane can maximally sustain the angle [17]

$$\tan \varphi = \sqrt{3(3\xi - 1)/(2 + 3\xi)}, \quad (16)$$

a typical angle of $\varphi_c = 28^\circ$ implies $\xi = 5/3$.

We concentrate on cohesionless dry sand here, though the same approach applies to wet sand as well. Adding $-P_c\Delta$ with $P_c > 0$ to the energy w , i.e., taking the energy to be $w^{\text{wet}} = w - P_c\Delta$, does not alter the convexity condition Eq. (15), only changes the expression for the measured pressure,

$P^{\text{wet}} \equiv \partial w^{\text{wet}}/\partial \Delta = P - P_c$, where $P \equiv \partial w/\partial \Delta$. As a result, Eq. (15) assumes the Mohr-Coulomb form,

$$\sigma_s/(P^{\text{wet}} + P_c) = \sqrt{2\xi}. \quad (17)$$

The second derivative of the energy w yields the stiffness tensor, $M_{ijkl} \equiv \partial \sigma_{ij}/\partial u_{kl} \equiv -\partial^2 w/\partial u_{ij}\partial u_{kl}$, while the compliance tensor, $\lambda_{ijkl} \equiv \partial u_{ij}/\partial \sigma_{kl}$, is the inverse of M_{ijkl} . Both are surprisingly complicated and anisotropic expressions. In the so-called ‘‘principle system’’ of coordinates, in which σ_{ij} is diagonal, they are given as (see the second reference in Ref. [18])

$$M_{ijkl} = \mathcal{A}\sqrt{\Delta} \left[\left(u_s^2/4\Delta^2 + \frac{4}{3} - \frac{3}{2}B/\mathcal{A} \right) \delta_{ij}\delta_{kl} - \delta_{ik}\delta_{jl} - \delta_{il}\delta_{jk} + (u_{ij}\delta_{kl} + \delta_{ij}u_{kl})/\Delta \right] \quad (18)$$

$$= \mu \left[\left(\frac{\mathcal{A}^4\sigma_s^2}{16\mu^6} + \frac{2}{3} - \frac{3B}{2\mathcal{A}} \right) \delta_{ij}\delta_{kl} - \delta_{ik}\delta_{jl} - \delta_{il}\delta_{jk} - \frac{1}{2}\mathcal{A}^2(\sigma_{ij}^0\delta_{kl} + \sigma_{kl}^0\delta_{ij})/\mu^3 \right], \quad (19)$$

$$\lambda_{ijkl} = \frac{[\mathcal{A}u_s^2 + 2(\mathcal{A} - B)\Delta^2]\delta_{kl}\delta_{ij}}{6\mathcal{A}\sqrt{\Delta}(\mathcal{A}u_s^2 - 2B\Delta^2)} - \frac{\delta_{ik}\delta_{jl} + \delta_{il}\delta_{jk}}{4\mathcal{A}\sqrt{\Delta}} + \frac{u_{ij}\Delta\delta_{kl} + u_{kl}\Delta\delta_{ij} + u_{ij}u_{kl}}{3\sqrt{\Delta}(\mathcal{A}u_s^2 - 2B\Delta^2)} = \frac{9\mathcal{A}^5\sigma_s^2 + (32\mathcal{A} - 72B)\mu^6}{54\mu(\mathcal{A}^5\sigma_s^2 - 8\mu^6B)}\delta_{kl}\delta_{ij} - \frac{\delta_{ik}\delta_{jl} + \delta_{il}\delta_{jk}}{4\mu} \quad (20)$$

$$- \frac{4\mathcal{A}^3\mu^3(\sigma_{ij}^0\delta_{kl} + \sigma_{kl}^0\delta_{ij}) - 3\mathcal{A}^5\sigma_{ij}^0\sigma_{kl}^0}{9\mu(\mathcal{A}^5\sigma_s^2 - 8\mu^6B)}, \quad (21)$$

where the respective first expression is strain-dependent, the second stress dependent. The shear moduli μ of Eq. (12), if taken as stress dependent, is given as

$$\mu \equiv \mathcal{A}\{[1 + \sqrt{1 - (B/2\mathcal{A})(\sigma_s^2/P^2)}]P/2B\}^{1/3}. \quad (22)$$

Due to the circumstance discussed around Eq. (8) about ‘‘incremental nonlinearity,’’ M_{ijkl} or λ_{ijkl} can be compared to experiments directly. The data collected by Kuwano and Jardine [5] are extensive, comprising of 36 components of the compliance tensor (21 ones if the tensor is assumed symmetric), all as functions of pressure, shear and the void ratio e . Comparing these data to Eq. (21) is an ambitious test: The theory only depends on two material parameters, B_0 and ξ , with the latter essentially fixed by the yield condition, Eq. (15). As mentioned, we take $\xi = 5/3$. So only B_0 , the scale factor and measure of total stiffness, is left as an adjustable parameter. Taking $B_0 = 8500$ MPa and 7000 MPa, we find satisfactory agreement, see second reference of Ref. [18], with their data on Ham river sand and ballotini (glass beads), respectively, at all values of pressure, shear, and void ratio—

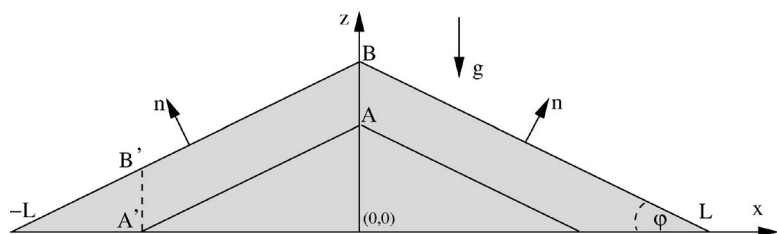


FIG. 1. A sand wedge. Its profile at an earlier moment of formation is shown by the line $A-A'$. Note that if the pile is formed by grains being funneled onto the peak, those arriving at B' have met similar circumstances and undergone comparable motions as those arriving at A' previously.

except very close to yield where plastic contributions are significant.

This clear experimental support for the compliance tensor λ_{ijkl} (or equivalently for the stiffness tensor M_{ijkl}) is an equally strong support for the elastic-strain-stress relation, Eqs. (11) and (12), because the latter is an integration of M_{ijkl} , over the sum of elastic increments from successive stress points. The finite displacement thus obtained is the mathematical path that a system could take to achieve the given stress state without any plastic contributions, though it rarely, if ever, does this. Nevertheless, it is completely appropriate for closing the force balance and evaluating static stress distributions in granular systems. This is what we shall do next, and in the accompanying paper, to check whether this stress-strain relation holds up under circumstances where the stress, and in one case also the density, are nonuniform. As the calculation does not contain any fit parameters, even qualitative agreements with experiments would be satisfactory, though they are generally better.

There is no fit parameter, because (a) $\xi=5/3$, and (b) as a scale factor, the elastic coefficient B_0 does not influence the stress (provided the boundary conditions either are given in terms of stresses or require that the displacement vanishes). The reason is, given a solution, one may change the strain by the factor α , and B_0 by $\alpha^{-1.5}$, with the stress unchanged and still a solution. That stress distributions do not depend on the stiffness, and remain equal for rubber and granite grains if they share the same Coulomb yield angle, is a remarkable consequence of the energy w in Eq. (10). Whether it is a good approximation is a question worthy of some experimental scrutiny.

As a corollary, the stress distribution does not depend on the value of a uniform void ratio e , as it only corresponds to changing the scale of B_0 . But a nonuniform e , as discussed, does make a difference, via a term $\sim \nabla \rho$.

Finally, we discuss the connection of GE (granular elasticity) to granular statistical mechanics (GSM), an idea Edwards [20] developed nearly two decades ago that is an active area today. GE starts from the usual thermodynamic relation, taking the energy density as a function of the densities of entropy s , mass ρ and strain u_{ij} ,

$$dw = Tds + \mu d\rho + \sigma_{ij} du_{ij}. \quad (23)$$

The chemical potential μ and the stress σ_{ij} may be calculated from Eq. (10), in which the entropy dependence (taking $T \rightarrow 0$) is neglected. (Denoting f_1 as the free energy, and m as the mass, per grain, we note in Ref. [17] that there is a contribution $\rho f_1/m$ to the free energy density. The entropy dependence may be calculated from it.)

Taking the grains to be infinitely rigid, $u_{ij} \equiv 0$, GSM starts from the observation that packaging them (which neither attract nor repel each other) will yield rather different densities, but will always maintain a vanishing energy, $dw \equiv 0$. These two relations reduce Eq. (23) to $d\rho = -(T/\mu)ds$. (Note both T and μ vanish in the considered limit, though their ratio may be finite.) Switching to extensive variables and keeping the volume V constant, this relation may be written as $dM = -(T/\mu)dS$, where $M \equiv V\rho$ is the mass and $S \equiv sV$ the entropy. For constant M (or equivalently, constant number of particles), we have instead

$$dV = XdS, \quad X \equiv T/(\mu\rho + Ts). \quad (24)$$

The first is the starting equation of GSM, where e^S is the number of possible configurations, all equally probable and energetically degenerate, but of varying density.

We choose to work with Eq. (23), because grains are, irrespective of the material's rigidity, infinitely pliable for $\Delta \rightarrow 0$, see Eq. (12). And the energy w is finite for deformable grains.

VII. STRESS DISTRIBUTIONS IN SAND PILES

The fact that the pressure distribution below sand piles and wedges, instead of always displaying a single central peak, may sometimes show a dip, has in its implication [14] intrigued and fascinated many physicists in the past decade, prodding them to think more carefully and deeply about sand. Recent experimental investigations established the following connection: A single peak results when the pile is formed by rainlike pouring from a fixed height; the dip appears when the pile is formed by funneling the grains onto the peak, from a shifting funnel always hovering slightly above the peak, see Refs. [10,21] for experimental evidences and a well-rounded review including many references. A yes-no phenomenon, this connection is accepted as a clear evidence for the preparation dependence of granular stresses. The ability to shed some light on this phenomenon is one of the crucial tests for a theory aiming to yield a broad, generally valid, qualitative understanding of granular statics. Therefore, we employ GE to investigate two-dimensional sand piles in this section.

A. Granular elasticity with varying density

Assuming two dimensionality—zero displacement, strain and stress in the y direction—we consider the sand wedge as shown in Fig. 1. Rewriting Eqs. (10) and (11) slightly, we find the elastic energy w and the stress $\sigma_{ij} = -\partial w / \partial u_{ij}$ given as

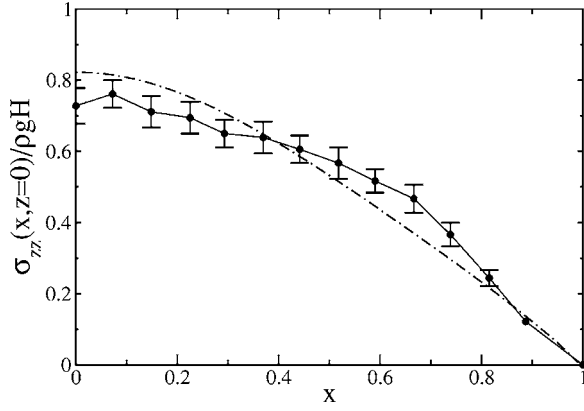


FIG. 2. Normalized pressure at the bottom of a wedge ($\rho g H$ is the maximal hydrostatic pressure) versus the horizontal coordinate x . Dashed-dotted line, granular elasticity; circles with error bars, experiment with rainlike pouring [21].

$$w = \sqrt{\Delta} \left(\frac{2}{5} B \Delta^2 + \mathcal{A} u_s^2 \right) = \mathcal{A} \sqrt{\Delta} \left(\frac{2}{5} \xi \Delta^2 + u_s^2 \right), \quad (25)$$

$$\sigma_{ij} = \mathcal{A} \left[\sqrt{\Delta} (\xi \Delta \delta_{ij} - 2u_{ij}^0) + \frac{1}{2} u_s^2 / \sqrt{\Delta} \delta_{ij} \right], \quad (26)$$

Both below and in the accompanying paper [3], we take $\xi \equiv B/\mathcal{A} = 5/3$, as it is fixed by the yield angle, and $\mathcal{A}_0 \equiv 5100$ Mpa, where \mathcal{A}_0 is defined by

$$\mathcal{A} = \mathcal{A}_0 \mathcal{A}_e, \quad \mathcal{A}_e \equiv (2.17 - e)^2 / [1.37(1 + e)]. \quad (27)$$

(The same information was given above, though in terms of $B \equiv \xi \mathcal{A} = 5\mathcal{A}/3$ rather than \mathcal{A} . Note that as a scale factor, \mathcal{A}_0 does not enter the stress distribution.)

Considering first the case of constant e , we inset Eq. (26) into the force balance $\nabla_j \sigma_{ij} = \rho g_i$ to calculate the stress numerically. The result is a single central peak, see Fig. 2, where it is compared to the experimental data obtained by the rainlike pouring procedure. (Following the authors of Ref. [21], we expect rainlike pouring to produce a fairly uniform density. This is plausible and it consistently leads to agreement between granular elasticity and experiments, also for silos and the point loads [3].) Being accomplished without any fit parameters, the agreement depicted in Fig. 2 is already fairly remarkable.

Next, we recall the discussion of Sec. III, in which we concluded that (i) the force balance is an expression for the entropy being maximal with respect to strain variations, so there cannot be any frozen strain fields. Conversely, (ii) the density field is indeed frozen in when the grains get jammed, and this will contribute to preparation-dependent stress corrections. (iii) There may be additional macroscopic variables that have similar effects as the density. But before making granular elasticity more complicated, it is sensible to first establish some unambiguous evidence for the necessity of including them. It is in this vein that we aim to account for the above-mentioned preparation dependence of granular stresses by employing granular elasticity with an assumed density inhomogeneity, to see whether its effect and magnitude are at all compatible with experimental findings.

Currently, we have no way of knowing what density field the funneling procedure produces—this being the realm of

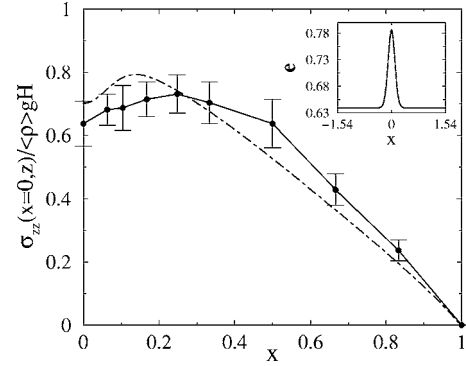


FIG. 3. Normalized pressure at the bottom of a wedge. Dashed-dotted line, theory; circles with error bars, experiment [21]. Inset, the assumed void ratio field $e(x)$ of Eq. (35).

dynamics and plastic strains. But as depicted and captioned in Fig. 1, the density at the points A' , B' should be similar, so the main density variation is horizontal, not vertical. With the shifting funnel hovering slightly above the peak, the grains have been deposited there with very little kinetic energy. Therefore, the density in a small region around the peak should be fairly close to the random loosest value, $e \approx 0.8$. Further away, the grains gathered kinetic energy while rolling down the slope, achieving a greater compactness when they crashed to a stop. Assuming for simplicity a two-density model: a loose center ($e \approx 0.78$) and two compact flanks ($e \approx 0.64$, an 8% density increase), with a soft transition between them, we were able to adjust the size of the center and the magnitude of the density change to produce a dip comparable to the measured one, see Fig. 3. Although the density field is assumed, and the agreement slightly strained, this result shows, at the very least, that stress corrections from density variations are of sufficient magnitude to account for typical experimental findings. And this does render the hypothesis they are the main cause for preparation dependence rather more probable.

B. Equations and numerical method

The details of solving the differential equations using the finite difference method are reported next. First, we introduce dimensionless quantities, though we do keep the same symbols. We take all lengths to be given in units of H , the height of the sand pile, and the stress in units of \mathcal{A}_0 [see Eq. (27)]: $z \rightarrow z/H$, $x \rightarrow x/H$, $U_i \rightarrow U_i/H$, and $\sigma_{ij} \rightarrow \sigma_{ij}/\mathcal{A}_0$, where especially $H=1$, and $L=1/\tan \varphi$ (φ is the angle of the slope, see Fig. 1).

Substituting Eq. (26) into the force balance, the following second-order partial differential equations for the displacements U_x, U_z are obtained

$$\mathcal{L}_x = 0, \quad \mathcal{L}_z = -2\beta \Delta^{3/2}, \quad (28)$$

where denoting $\Delta \equiv -(\partial_x U_x + \partial_z U_z)$, $\kappa \equiv \partial_x U_z + \partial_z U_x$, we have β , dimensionless and preceding the only nonanalytical term $\sim \Delta^{3/2}$ of the differential equations,

$$\beta = \rho g H / \mathcal{A}_0 \quad (29)$$

and

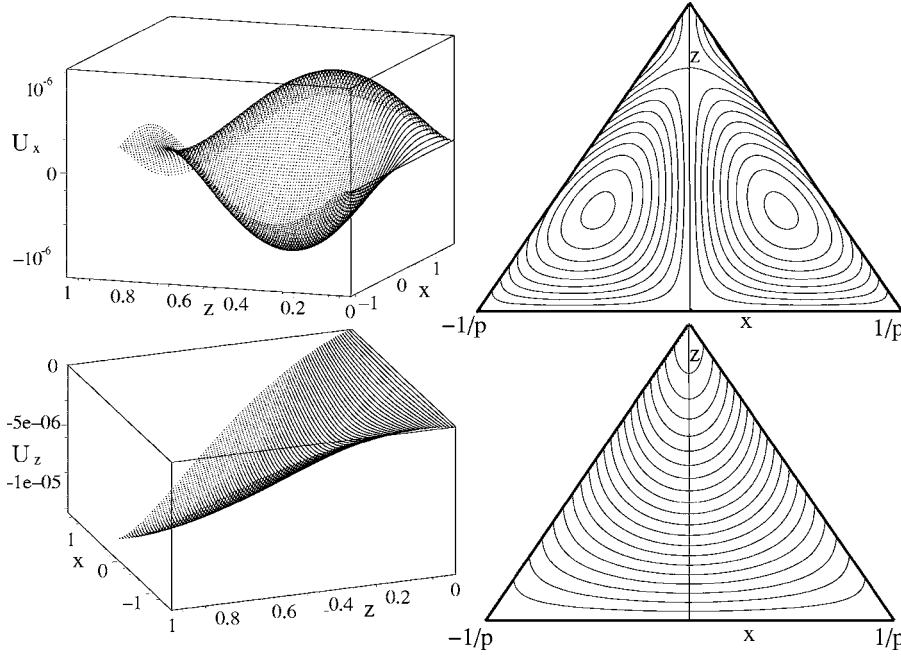


FIG. 4. (a) The normalized x and z components of the displacements inside a sand pile with contour lines of corresponding surfaces.

$$\begin{aligned}
 \mathcal{L}_x = & -2\Delta^2 \partial_z^2 U_x + \kappa \Delta (\partial_x^2 U_z + \partial_z^2 U_x) + \left[\left(\frac{\Delta}{2} + \partial_z U_z \right)^2 - 3\Delta^2 \xi \right. \\
 & \left. + \frac{\kappa^2}{4} \right] \partial_x \partial_z U_z + 2\kappa \Delta \partial_x \partial_z U_x + \left[\left(\frac{3\Delta}{2} - \partial_z U_z \right)^2 - 3\Delta^2 (2 \right. \\
 & \left. + \xi) + \frac{\kappa^2}{4} \right] \partial_x^2 U_x + 2\Delta \left[\frac{\partial_x \mathcal{A}_e}{\mathcal{A}_e} \left(\Delta [\Delta (\xi - 1) - 2\partial_x U_x] \right. \right. \\
 & \left. \left. + \frac{u_s^2}{2} \right) - \frac{\partial_z \mathcal{A}_e}{\mathcal{A}_e} \kappa \Delta \right], \quad (30)
 \end{aligned}$$

with \mathcal{L}_z obtained from \mathcal{L}_x by interchanging the indices, $\mathcal{L}_z = \mathcal{L}_x(x \leftrightarrow z)$.

Six boundary conditions, two at every surface, are needed. At the bottom, we take the grains to be glued,

$$U_x|_{z=0} = U_z|_{z=0} = 0. \quad (31)$$

Although the inclined surfaces ($z=1 \pm x \tan \varphi$) are free, we need to take them subject to a small normal force P_c , or $\sigma_{ik} n_k = n_i P_c$. This is because granular elasticity contains the Coulomb yield, and a completely free surface, $\Delta \rightarrow 0$, though analytically stable, tends to give rise to numerical divergencies. As the assumed P_c will turn out two orders of magnitude smaller than σ_{ij}^{\max} , the maximal value of the calculated stress, we do not expect its presence to alter the result in any significant way. (Note that this P_c may equivalently be associated with some residual cohesion of the sand.) So the boundary conditions for the left ($z=1+x \tan \varphi$) and right ($z=1-x \tan \varphi$) surfaces are, respectively,

$$\sigma_{xx} - \sigma_{xz}/\tan \varphi = P_c, \quad -\sigma_{xz} \tan \varphi + \sigma_{zz} = P_c, \quad (32)$$

$$\sigma_{xx} + \sigma_{xz}/\tan \varphi = P_c, \quad \sigma_{xz} \tan \varphi + \sigma_{zz} = P_c. \quad (33)$$

This system of coupled second-order partial differential equations including the six specified boundary conditions are solved numerically by the finite-difference method, using a homogeneous grid for the sand pile. First, a system of nonlinear algebraic equations for U_x, U_z at the nodes of the grid are set up using a Fortran code, then an initial guess is made for all nodes, and a solution is arrived at by iterating it until the values are stationary, typically after 10^5 iterations. Finally, the results are verified by independent FEMLAB calculations.

Note that after the solution is found for a given value of β [see Eq. (29)], the solution for any value of $\beta \rightarrow \beta/\gamma$ can be found by

$$U_i \rightarrow \frac{U_i}{\gamma^{2/3}}, \quad \sigma_{ij} \rightarrow \frac{\sigma_{ij}}{\gamma}, \quad P_c \rightarrow \frac{P_c}{\gamma}. \quad (34)$$

C. Results for uniform densities

First, we assume a uniform density, taking the density of the granular material as $\rho_g = 2600 \text{ kg/m}^3$, and the void ratio as $e = 0.66$, the granular density is $\rho/\rho_g = 1/(1+e) = 0.60$. The height of the sand pile is taken as $H = 8 \text{ cm}$, and the slope angle as $\varphi = 33^\circ$, both same as in the experiment [21]. We also take $\mathcal{A}_0 = 5100 \text{ Mpa}$, a quantity that will not change the stress, but does influence the strain. As a result, we have $\beta = 2.4 \times 10^{-7}$.

Figure 4 shows the displacement U_x and U_z . Obviously, there is a reflection symmetry with respect to the x direction, and U_x and U_z are, respectively, antisymmetric and symmetric with respect to x . If the left-hand part of a sand pile ($x \leq 0$) is contracted along x , this is also the case on the right-hand part ($x \geq 0$). Conversely, both parts are equally contracted in the z direction. In addition, we have $U_x(x=0, z) = 0$ and $\partial_z U_x(x=0, z) = \partial_x U_z(x=0, z) = 0$ for $x=0$, which leads to $\sigma_{xz}(x=0, z) = 0$. Taking into account the fact

that the top of the sand pile belongs to both boundaries, one finds $\partial_x U_x(x=0, z=1) = \partial_z U_z(x=0, z=1) = -1/2(P_c/\xi)^{2/3}$. The z component of the displacement is negative, $U_z \leq 0$, and its maximum is an order of magnitude larger than that of U_x , which is a result of the gravitational force. Note that for the left-hand part of the pile we have $U_x > 0$ for $z \geq 0.7$, $U_x < 0$ for $z \leq 0.7$, and vice versa for the right-hand part. In other words, the upper part of a sand pile contracts along x , and the lower part expands.

As pointed out, P_c is introduced to avoid numerical divergencies on the free surfaces. Reassuringly, it is found to be much smaller than the maximal pressure, $\max(\sigma_{zz})/P_c \sim 77$.

D. Results for nonuniform density

Next, we assume the nonuniform density given as

$$\rho = \rho_0 + b(1 - e^{-c^2 x^2}), \quad b = \frac{\rho_L - \rho_0}{1 - e^{-c^2/\tan^2 \varphi}}. \quad (35)$$

It describes a two-region model, with $\rho = \rho_0$ at the center ($cx \ll 1$), and $\rho = \rho_L$ at the flanks ($cx \gg 1$). We take $\rho_0/\rho_g = 0.56$ (that corresponds to the void ratio of $e = 0.786$, fairly close to the maximal value of 0.8) and $\rho_L/\rho_g = 0.61$ (or $e = 0.639$). Taking in addition $c = \sqrt{50}$, the transition occurs around $x = 1/\sqrt{50} \approx 0.14$, see Fig. 3. The results, never far from the error bars, show a clear dip. [Note $\sigma_{zz}/\langle \rho \rangle gH$ is shown, where $\langle \rho \rangle \equiv \int_S \rho(x, z) dx dz / S$.]

VIII. SUMMARY

Our starting point is the observation that although in granular media, grains may slide and roll, in addition to being compressed and sheared, only the latter, the deformation of the grains, leads to reversible energy storage, while sliding and rolling at most heat up the system. Therefore, we postulate the existence of an “elastic displacement” U_i , which is what remains if sliding and/or rolling are eliminated from the actual displacement field. Calculating from it the “elastic strain field” u_{ij} , we take the deformation energy w to depend on u_{ij} —rather than the much larger, total strain field ε_{ij} . The field U_i is rarely, or never, equal to the observed, total displacement field in a granular system, however carefully it was prepared, but it is the one mathematically possible, fully reversible path to achieve the given stress. This is why the stress is $\sigma_{ij}(u_{kl}) = \partial w / \partial u_{ij}$, reflecting its dependence on the deformation of the grains, rather than the amount of rolling and/or sliding in the system’s past. This approach has a number of immediate consequences:

(1) Any expression for w yields a strain-stress relation, $\sigma_{ij} = \sigma_{ij}(u_{kl})$, equivalently $\dot{\sigma}_{ij} = (\partial \sigma_{ij} / \partial u_{kl}) \dot{u}_{kl}$. Yet this has no implication for the observed strain rate, $\dot{\varepsilon}_{kl}$. It is the hyperelastic model, $\dot{\sigma}_{ij} = (\partial \sigma_{ij} / \partial \varepsilon_{kl}) \dot{\varepsilon}_{kl}$, that contradicts “incremental nonlinearity,” GE does not. Neither does GE imply smooth deformations, or rules out adaptation of force chains and irreversible, plastic repackaging.

(2) Taking the plastic part of the strain rate as $\dot{u}_{kl}^p \equiv \dot{\varepsilon}_{kl} - \dot{u}_{kl}$, we may write $\dot{\sigma}_{ij} = (\partial \sigma_{ij} / \partial u_{kl}) (\dot{\varepsilon}_{kl} - \dot{u}_{kl}^p)$, and compare it to the hypoplastic model [4], $\dot{\sigma}_{ij} = M_{ijkl} \dot{\varepsilon}_{kl} - N_{ij} \sqrt{\dot{\varepsilon}_{kl} \dot{\varepsilon}_{kl}}$.

Clearly, it is the plastic term, $\dot{u}_{mn}^p = (\partial u_{mn} / \partial \sigma_{ij}) N_{ij} \sqrt{\dot{\varepsilon}_{kl} \dot{\varepsilon}_{kl}}$, that gives rise to incremental nonlinearity.

(3) As the relation $\sigma_{ij} = \sigma_{ij}(u_{kl})$ expresses σ_{ij} in terms of the three components of U_i , it closes the force balance, $\nabla_j \sigma_{ij} = \rho g_i$, and represents a systematic, geometry-independent procedure for calculating static granular stresses.

(4) When probing the strain response $\delta \varepsilon_{ij}$ to a stress increment $\delta \sigma_{kl}$, measuring the relation $\delta \sigma_{ij} = M_{ijkl} \delta \varepsilon_{kl}$, incremental nonlinearity is known to vanish with the amplitude of the increments, or $\delta \varepsilon_{ij} \approx \delta u_{ij}$ for $\delta \varepsilon_{ij} \rightarrow 0$. (It is probably due to the fact that sliding and/or rolling decrease dramatically in the limit of vanishing increments.) This is useful, because $\delta \sigma_{ij} = (\partial \sigma_{ij} / \partial u_{kl}) \delta u_{kl} \approx (\partial \sigma_{ij} / \partial u_{kl}) \delta \varepsilon_{kl}$, and we can identify M_{ijkl} with $\partial \sigma_{ij} / \partial u_{kl} = \partial^2 w / \partial u_{ij} \partial u_{kl}$ for $\delta \varepsilon_{ij} \rightarrow 0$, implying that all 36 components of M_{ijkl} may be obtained from the energy w , a scalar.

(5) Taking (a) the constitutive relation to depend on the density, $\sigma_{ij} = \sigma_{ij}(u_{kl}, \rho)$, and (b) the density being quenched at preparation yields a natural explanation for the preparation dependence of the stress. The elastic strain u_{kl} is not quenched: slightly displacing a volume element by exerting a force there, the element will return to its original spot when let go, with some overshooting first. This damping of sound waves is the visible approach of u_{kl} to its equilibrium value, $\nabla_j \sigma_{ij} = 0$.

(6) A static solution obtained employing $\nabla_j \sigma_{ij} = 0$ is an extremum of the energy $\int w d^3 r$. The solution is stable with respect to fluctuations (and the medium is jammed), if this extremum is a minimum and the fluctuations cost energy. This happens when w is a convex function of u_{ij} , and the eigenvalues of $M_{ijkl} = \partial \sigma_{ij} / \partial u_{kl}$ (as a 6×6 matrix) are all positive. If any eigenvalue turns negative, the extremum becomes a maximum in the direction of the associated eigenvector. Then no static stress distribution is possible, because stress fluctuations will form spontaneously in this direction to lower the energy. The system is no longer jammed and starts moving. Therefore, we identify the yield line as the boundary in stress space where w turns concave.

The actual expression we choose for the energy, Eq. (10), contains two material parameters, \mathcal{A} and \mathcal{B} . It does not allow negative compression, accounting for the lack of tensile forces in dry sand, and it turns concave at the (Drucker-Prager variant) of the Coulomb yield line, for $\sigma_s / P = \sqrt{2} \mathcal{A} / \mathcal{B}$.

We calculated $\partial \sigma_{ij} / \partial u_{kl} = \partial^2 w / \partial u_{ij} \partial u_{kl}$, and compared the results to the 36 elements of M_{ijkl} , measured by Kuwano and Jardine. As reported [18], rather satisfactory agreement is found. Since the ratio $\mathcal{A} / \mathcal{B}$ is already fixed by the yield line, leaving only \mathcal{B} (a scale factor and measure of total stiffness) to improve the fit, this agreement is a tribute to the chosen w . More importantly, the agreement provides a retrospective proof for the existence of the postulated elastic displacement U_i : We may now integrate over the stress increments, $u_{ij} = \int (\partial u_{ij} / \partial \sigma_{kl}) d\sigma_{kl}$, from zero to the given stress, with $(\partial u_{ij} / \partial \sigma_{kl})$ taken from the Kuwano and Jardine data, to obtain u_{ij} , and hence U_i , for any finite stresses.

If we take \mathcal{B} (but not $\mathcal{B} / \mathcal{A}$) to depend on the density as given by Eq. (14), then $\partial \sigma_{ij} / \partial u_{kl} = \partial^2 w / \partial u_{ij} \partial u_{kl}$ reproduces

$M_{ijk\ell}$ not only as a function of the stress, but also of the density. This is as such of course a welcome result, but it also fixes the density dependence of the constitutive relation, $\sigma_{ij} = \sigma_{ij}(u_{k\ell}, \rho)$, leaving no wiggle room when the preparation dependence of the stress is calculated for given density.

In Sec. VII and the accompanying paper, we employ this theory to calculate the stress distributions in three classic geometries: silos, point loads, and sand piles. Taking \mathcal{B} as given by Eq. (13) and $\mathcal{B}/\mathcal{A}=5/3$, the theory is without any fit parameter. Nevertheless, we were well able to account for all measured data in these geometries, and uncovered some interesting, perhaps even important points, one in each case:

(i) In silos, the Janssen ratio $k_J = \sigma_{rr}/\sigma_{zz}$ is found to be constant and given by the Jaky formula, $k_J = 1 - \sin \varphi$, where

φ denotes the Coulomb angle. This demonstrates that φ is a relevant parameter for the stress distribution even away from yield.

(ii) When sheared granular layers are subject to a point load, measurable anisotropy results. Typically interpreted as frozen-in, it is shown to be reversible and stress induced.

(iii) Sand piles display a central dip in its pressure when specially prepared. We are able to reproduce it by starting from a density profile that could plausibly result from the given preparation. This demonstrates granular elasticity's viability to account for the history dependence of granular stresses. (Density is not being scrutinized much at the moment, but it is measurable in experiments and calculable in simulations.)

-
- [1] M. E. Cates, J. P. Wittmer, J.-P. Bouchaud, and P. Claudin, *Chaos* **9**, 511 (1999).
- [2] L. D. Landau and E. M. Lifshitz, *Theory of Elasticity*, 3rd ed. (Pergamon, New York 1986).
- [3] K. Bräuer, M. Pfitzner, D. O. Krimer, M. Mayer, Y. Jiang, and M. Liu, following paper, *Phys. Rev. E* **74**, 061311 (2006).
- [4] D. Kolymbas, in *Introduction to Hypoplasticity* (Balkema, Rotterdam, 2000).
- [5] R. Kuwano and R. J. Jardine, *Geotechnique* **52**, 727 (2002).
- [6] F. Alonso-Marroquin and H. J. Herrmann, *Phys. Rev. Lett.* **92**, 054301 (2004). Note that their conclusion of the absence of an elastic regime pertains to the observation that the plastic response adds up over the long run, while the dominant elastic response averages to zero.
- [7] L. Vanel, D. Howell, D. Clark, R. P. Behringer, and E. Clément, *Phys. Rev. E* **60**, R5040 (1999).
- [8] G. Reydellet and E. Clément, *Phys. Rev. Lett.* **86**, 3308 (2001).
- [9] D. Serero, G. Reydellet, P. Claudin, E. Clément, and D. Levine, *Eur. Phys. J. E* **6**, 169 (2001).
- [10] A. P. F. Atman, P. Brunet, J. Geng, G. Reydellet, P. Claudin, R. P. Behringer, and E. Clément, *Eur. Phys. J. E* **17**, 93 (2005).
- [11] M. Otto, J.-P. Bouchaud, P. Claudin, and J. E. S. Socolar, *Phys. Rev. E* **67**, 031302 (2003).
- [12] R. M. Nedderman, *Statics and Kinematics of Granular Materials* (Cambridge University Press, Cambridge, England, 1992).
- [13] H. A. Janssen, *Dtsch. Eng.* **39**, 1045 (1895).
- [14] J. Wittmer, P. Claudin, M. E. Cates, and J.-P. Bouchaud, *Nature* (London) **382**, 336 (1996); J. Wittmer, M. E. Cates, and P. Claudin, *J. Phys. I* **7**, 39 (1997); M. E. Cates, J. P. Wittmer, J. P. Bouchaud, and P. Claudin, *Phys. Rev. Lett.* **81**, 1841 (1998).
- [15] C. Goldenberg and I. Goldhirsch, *Phys. Rev. Lett.* **89**, 84302 (2002).
- [16] J. Geng, D. Howell, E. Longhi, R. P. Behringer, G. Reydellet, L. Vanel, E. Clément, and S. Luding, *Phys. Rev. Lett.* **87**, 35506 (2001).
- [17] Yimin Jiang and Mario Liu, *Phys. Rev. Lett.* **91**, 144301 (2003); **93**, 148001 (2004); a slightly more complicated elastic energy $w = \frac{2}{5}B\Delta^{2+b} + A\Delta^a u_s^2$, was considered in the first reference. Weighing accuracy versus simplicity, we find the improvements achieved by allowing a, b , to deviate from each other not worth the loss of analytic manipulability. Taking $a=b \sim \frac{1}{2}$, implying $K, \mu \sim P^{1/2}$, would perhaps better reflect the acoustic data, though be less appropriate with respect to the yield. More complex energy expressions may well be needed for quantitative investigations, but the general strategy of the present approach should remain valid. Note $\mathcal{A} = \tilde{K}_a = \frac{1}{2}\mathcal{A}$, $\mathcal{B} = \frac{5}{4}\tilde{K}_b = \frac{5}{4}\mathcal{B}$.
- [18] *Powders and Grains 05*, edited by R. Garcia-Rojo, H. J. Herrmann, and S. McNamara (Belkema, Rotterdam, 2005), p. 433.
- [19] B. O. Hardin and F. E. Richart, *J. Soil Mech. and Found. Div.* **89**, 33 (1963).
- [20] S. F. Edwards and R. B. S. Oakeshott, *Physica A* **157**, 1080 (1989).
- [21] L. Vanel, D. Howell, D. Clark, R. P. Behringer, and E. Clément, *Phys. Rev. E* **60**, R05040 (1999).